1-2015

Girder Load Distribution for Seismic Design of Integral Bridges

Justin Vander Werff
Dordt College, justin.vanderwerff@dordt.edu

Sri Sritharan
Iowa State University

Recommended Citation

Vander Werff, J. and Sritharan, S. (2015). "Girder Load Distribution for Seismic Design of Integral Bridges." J. Bridge Eng., 20(1), 04014055.

Girder Load Distribution for Seismic Design of Integral Bridges

Abstract

Current seismic design practice related to integral bridge girder-to-cap beam connections allows little or no lateral seismic load to be distributed beyond the girders immediately adjacent to the column. However, distribution results from several large-scale tests have shown that the distribution of column seismic moment typically engages all the girders. An approach utilizing simple stiffness models to predict distribution in integral bridge structures is presented in detail; distribution predictions based on grillage analyses also are compared. The experimental results and the analytical results from the stiffness and grillage models show that current design methods related to vertical load distribution are sufficiently accurate. However, when applied to the distribution of lateral load, similarly obtained results reveal that current design practice does not appropriately account for the amount of load that is distributed beyond the girders adjacent to the column to the nonadjacent girders. The current practice leads to excessive girder-to-cap connection reinforcement, increased girder depth, unnecessarily high seismic mass, and increased construction cost. Finally, this paper makes recommendations for more appropriate distribution of seismic lateral load in integral bridge superstructures.

Keywords

seismic analysis, seismic design, girder bridges, load distribution, lateral forces, earthquake engineering, bridge loads

Disciplines

Civil Engineering

Girder Load Distribution for Seismic Design of Integral Bridges

Justin Vander Werff[1], P.E., M.ASCE and Sri Sritharan[2], M.ASCE

Abstract

Current seismic design practice related to integral bridge girder-to-cap beam connections allows little or no lateral seismic load to be distributed beyond the girders immediately adjacent to the column. However, distribution results from several large-scale tests have shown that the distribution of column seismic moment typically engages all the girders. An approach utilizing simple stiffness models to predict distribution in integral bridge structures is presented in detail; distribution predictions based on grillage analyses are also compared. The experimental results and the analytical results from the stiffness and grillage models show that current design methods related to vertical load distribution are sufficiently accurate. However, when applied to the distribution of lateral load, similarly-obtained results reveal that current design practice does not appropriately account for the amount of load that is distributed beyond the girders adjacent to the column to the non-adjacent girders. The current practice leads to excessive girder-to-cap connection reinforcement, increased girder depth, unnecessarily high seismic mass, and increased construction cost. Finally, this paper makes recommendations for more appropriate distribution of seismic lateral load in integral bridge superstructures.

Keywords

Seismic analysis, Seismic design, Girder bridges, Load distribution, Lateral forces, Earthquake engineering, Bridge loads

[1] Assistant Professor, Dordt College, Engineering Department, Justin.VanderWerff@dordt.edu, 498 4th Ave NE, Sioux Center, IA 51250

[2] Wilson Engineering Professor, Iowa State University, Department of Civil, Construction, and Environmental Engineering, sri@iastate.edu, 394 Town Engineering, Ames, IA 50011

Introduction

Integral bridges have several advantages over non-integral configurations. These advantages, which have been well-documented in recent years (Snyder et al. 2011, Maruri and Petro 2005, Wassef et al. 2004), have led to increased implementation of integral configurations, but design recommendations for such structures continue to be limited in some critical areas. The distribution of lateral load between girders in the superstructure is a particular aspect of integral bridge design that has not been addressed adequately. Common bridge design recommendations such as the AASHTO standards (AASHTO 2010; AASHTO 2009) provide very little information on the distribution of lateral seismic loads. Common standards used in seismic regions, such as *Seismic Design Criteria* (*SDC*, 2006) and *Bridge Design Aids* (*BDA*, 1995) from the California Department of Transportation (Caltrans) also do not provide a detailed approach for seismic lateral load distribution.

Investigations over the past fifteen years have explored seismic lateral load distribution in the superstructure of integral bridge systems. Holombo et al. (2000) briefly looked at lateral load distribution alongside other issues of interest related to use of precast concrete superstructures in seismic regions. National Cooperative Highway Research Program (NCHRP) Project 12-54 (Wassef et al. 2004, Sritharan et al. 2005, Vander Werff 2002) investigated lateral load distribution as part of a research effort examining seismic issues in bridges with steel superstructures and concrete substructures. These projects and others have mentioned the issues related to seismic lateral load distribution based on experimental data. However, the authors are not aware of any studies that systematically investigate seismic lateral load

distribution using comparisons of experimental test data and predictive analytical models to formulate improved design recommendations.

The investigations mentioned above primarily focused on the performance and sufficiency of bridge systems for high seismic regions. The studies utilized the construction and testing of large-scale experimental models of prototype integral bridge structures. The first test unit modeled a bridge with a 4-girder prestressed concrete superstructure (Holombo et al. 2000), using precast bulb-tee girders. This test unit is referred to as the precast bulb-tee (PBT) model. The next two test units were based on bridges with 4-girder steel superstructures (Wassef et al. 2004). These units are referred to as the steel pier cap (i.e., SPC1 and SPC2) models. A more recent study by Caltrans investigated a test unit consisting of a 5-girder prestressed concrete superstructure (Snyder et al. 2011) including an inverted-tee bent cap. This unit is referred to as the inverted-tee bent cap (ITB) model. Fig. 1 provides schematic details of the prototype structures for these investigations. All of the tests had specific areas of focus; however, common areas of interest can be summarized as: (1) the design of a prototype bridge utilizing integral connection details capable of withstanding seismic loading, (2) the experimental validation of these details using large-scale test specimens, and (3) the formation of suitable seismic design recommendations based on the analytical and experimental findings. This paper compiles the load distribution results from these experimental tests and compares them with predictions from grillage and simple stiffness models.

Current Design Practice

The current *AASHTO LRFD Bridge Design Specifications* (2010) includes a well-established procedure for using distribution factors to distribute moment and shear due to vertical loads to interior and exterior girders with concrete decks (Section 4.6.2.2.2). The distribution factors are based on the spacing, span, and longitudinal stiffness of the beams and the depth of the slab. The distribution factor approach has been shown to be reliable for vertical live load by many studies (Zokaie et al. 1991, Kim and Nowak 1997, Mabsout et al. 1999, Barr et al. 2001, and Cai 2005, for example). Recent work as part of NCHRP Project 12-26 has continued with this approach while simplifying the equations (Mertz 2007).

Caltrans' current approach to vertical live load distribution incorporates the recommendations from AASHTO. While slight variations are made for special situations (see "Concrete box girder live load distribution by Lanell for special loads" 1998, or *California Amendments to AASHTO LRFD Bridge Design Specifications* 2011, for example), the basis of the approach continues to be spacing, span, and section properties of the girders and deck. This approach is appropriate for distributing service-level live loads. However, it is not analogous to the vertical load distribution that occurs when the bridge structure is exercised by large displacements and experiences considerable cracking due to a large seismic event. Also, the AASHTO distribution factors are primarily intended for girder design. However, a primary focus of seismic load distribution, particularly in conjunction with the ever-increasing use of segmental construction and accelerated bridge construction, is the design of the connections. Therefore, a stiffness-based approach to vertical load distribution during large seismic displacements is introduced later in this paper. This approach is primarily intended for use in conjunction with a similar lateral load distribution model in determining seismic load paths through the superstructure.

Regarding lateral load distribution, Section 4.11.2 in the *AASHTO Guide Specifications for LRFD Seismic Bridge Design* (2009) stipulates the superstructure components and their connections "shall be designed to resist overstrength moments and shears of ductile columns." Section 8.10 in these guidelines goes on to address the capacity design of the superstructure for integral bent caps in reinforced concrete structures. These guidelines limit the distribution of the column overstrength moment to an effective width equal to the sum of the diameter of the column and the depth of the superstructure. This stipulation is graphically summarized in Fig. 2. The practical conclusion of this requirement is that the column overstrength moment can rarely, if ever, be distributed to the exterior girders in a system utilizing a single-column bent. The AASHTO guidelines do not allow the distribution of any portion of the column overstrength moment to the exterior girders for any of the four prototype structures considered in this study.

Focusing on Caltrans' approach to lateral load distribution, Chapter 5 of Caltrans' *BDA* (1995) offers no information in the *BDA* related to lateral load distribution. Section 7.2 in Caltrans' *SDC* follows the AASHTO recommendations for lateral distribution, while additionally recommending "the effective superstructure width can be increased at a 45^{o} angle [in plan] as [the distance increases] from the bent cap until the full section becomes effective." This modification is shown in Fig. 2. This stipulation does not allow the distribution of the lateral load to the exterior girders at the cap-to-girder connection for all the prototype structures considered in this study and all similar integral bridge configurations. However, lateral load distribution would be permitted in regions where the longitudinal distance from the cap beam exceeds the girder spacing, identified in Fig. 2 as d_g.

Analytical Approaches

Detailed analytical models of integral bridge superstructures such as those incorporating a finite element analysis (FEA) can be helpful in understanding load distribution between girders. The bridge superstructure, including girders and cap beam, can be modeled using FEA, and the model can be used to investigate load paths of both vertical load and horizontal seismic effects using the column overstrength moment (applied as a torsional load in the cap beam) through the superstructure. While a FEA can provide helpful results, they are typically cumbersome and time-consuming. A slightly simpler approach is to utilize a grillage model analysis (GMA). A GMA approach utilizes line elements for girder and cap beam elements, simplifying the modeling process while still providing opportunity to investigate the load paths through the superstructure. A third analysis approach uses member-stiffness-based calculations to approximate the distribution of gravity and seismic loads; this model is referred to as a simple stiffness model (SSM). The following sections provide an in-depth look at the analytical models used in this load distribution investigation.

SSM Background

The difference in load direction between vertical and horizontal loads produces differences in load transfer through a bridge superstructure. Vertical loads moving through the superstructure into the column will be transferred as flexural loads in both the girders and the cap beam. However, the column overstrength moment resulting from seismic lateral loads will produce both torsional and flexural actions in portions of the superstructure. These actions will include

torsional loads in the cap beam, positive flexural loads in the girders on one side of the cap beam, and negative flexural loads in the girders on the opposing side of the cap beam. To account for these stiffness differences, two different SSMs are used for a given prototype structure. The first SSM for each structure is used to determine the distribution of the vertical load among the girders in the superstructure. The second SSM for each structure is used to investigate the distribution of the column overstrength moment. While the actual distribution is a combination of both actions, the vertical and lateral distribution behavior is separated to simplify the analysis.

SSM for Vertical Load

Fig. 3a provides a schematic diagram of the vertical load distribution concept. This concept is used to analyze how the self-weight of the bridge transfers from the superstructure into the column, or vice versa, as a way to isolate this load behavior from the lateral load transfer occurring from large seismic accelerations. As such, the vertical load SSM presented here is not analogous to the commonly-used AAHSTO live load distribution factors for vertical load discussed earlier. The SSM is developed by estimating the appropriate stiffness of each of the individual elements, assuming rigid connections between the girder and cap, and developing an overall load distribution model. Because typical bridge superstructures tend to be symmetrical, calculating the stiffness for only half of each specimen is usually appropriate, as long as a suitable boundary condition is incorporated at the specimen centerline as shown in Fig. 3b.

The stiffness terms k_{iv} and k_{ev}, for the interior and exterior girders, respectively, are defined as the magnitudes of flexural stiffness for the composite girder-deck sections, modeled as beams

that are simply supported with concentrated vertical loads applied at their midspans, as shown in Fig. 3c. Thus, using principles of basic mechanics, k_{iv} and k_{ev} can be determined using:

$$k = 48E_gI_g / L_g^3 \quad (1)$$

where E_g is the modulus of elasticity of the girder material, I_g is the effective girder moment of inertia of either the interior or exterior girder, and L_g is the girder span length. I_g is based on the composite section of the girder and bridge deck, using cracked and uncracked concrete properties as appropriate. The resulting values of k_{iv} and k_{ev} will likely not be equal because of the difference in tributary deck areas for the interior and exterior girders.

The cap beam flexural stiffness, k_{cv}, is determined by modeling the cap beam as a fixed-end cantilever beam with a concentrated vertical load applied at the free end as shown in Fig. 3d, where the cantilever beam represents the portion of the cap beam between the interior girder and exterior girder. The relationship for k_{cv} is:

$$k_{cv} = 3EI_c / L_{ce} \quad (2)$$

where E_c is the modulus of elasticity of the cap beam material, I_c is the effective moment of inertia of the cap beam, and L_{ce} is the length of the cap beam between the interior girder and the exterior girder.

An appropriate combined stiffness relationship can be developed by observing that, for a given configuration, the combined behavior of the various structural members will contribute to the resistance of a load in a manner either simultaneously parallel or sequentially in series with other individual member stiffness components. For example, referencing Fig. 3b, the load P,

which is translated by the rigid center link, will be resisted in parallel by the flexural stiffness of the cap beam (k_{cv}) and the flexural stiffness of Girder A (k_{iv}), but the contribution of k_{cv} from the cap beam will occur in series with the contribution from the flexural stiffness of Girder B (k_{ev}). The total stiffness of two components resisting a load in parallel is found by simply summing the two stiffness values. The total stiffness of two components resisting a load in series is found by dividing the product of the stiffness values by the sum of the stiffness values. Therefore, the equivalent stiffness, k_{vert}, for the scenario represented in Fig. 3b is given by:

$$k_{vert} = (k_{ev}k_{cv}) / (k_{ev} + k_{cv}) + k_{iv} \quad (3)$$

using the stiffness terms defined in Eqs. 1 and 2. The combined behavior of the external portion of the cap beam and the exterior girder, excluding the contribution of the interior girder, can be represented as:

$$k_{ev+cv} = (k_{ev}k_{cv}) / (k_{ev} + k_{cv}) \quad (4)$$

To determine the load distribution among the girders, the fractional relationships of appropriate stiffness terms are used to determine the fractional load expected in a particular girder. For example, for a symmetrical four-girder integral structure with stiffness terms determined as described above, the vertical load will be carried through two load paths (one through the interior girder and one through the cap beam and exterior girder). Therefore, the fractional load distribution to the interior girder is:

$$DF_{int} = k_{vert} / (k_{vert} + k_{ev+cv}) \quad (5)$$

and the fractional load distribution to the exterior girder is:

$$DF_{ext} = k_{ev+cv} / (k_{vert} + k_{ev+cv}) = 1 - DF_{int} \quad (6)$$

The accuracy of this approach depends on the appropriateness of the individual stiffness values used. Much work has been completed related to appropriate section properties to use for reinforced concrete sections, and some of this work has been devoted specifically to the behavior of reinforced concrete under seismic loading (see especially Priestley et al. 1996). In this study, since seismic behavior is of primary importance, composite section properties were determined assuming cracked concrete properties. Accordingly, the contribution of concrete on the tension side of the neutral axis was neglected in the determination of flexural section properties, following Priestley's approach.

SSM for Lateral Load

The SSM for lateral load distribution can be used to determine the distribution of the column overstrength moment through the superstructure. A schematic of the horizontal load distribution concept is shown in Fig. 4a. Symmetry again typically allows a half-model, as shown in Fig. 4b. The column overstrength moment is represented here as a torsional load in the cap beam. The applicable stiffness values are k_{it} and k_{et} (interior and exterior girder flexural stiffness) and k_{ct} (cap beam torsional stiffness). The girder stiffness values are determined by the girder flexural behavior as shown in Fig. 4c. Cracked and uncracked concrete properties are of particular interest in these stiffness values, since the bridge deck is in tension on one side of the cap beam and compression on the other side. Since the girders on each side of the cap beam act in parallel with each other, the girder stiffness values are:

$$k = 3EI_{gu} / (L_g / 2) + 3EI_{gc} / (L_g / 2) \quad (7)$$

where I_{gu} is the moment of inertia considering the deck concrete to be uncracked and I_{gc} is the moment of inertia with cracked deck concrete. The torsional stiffness of the cap is determined based on the theoretical model shown in Fig. 4d, resulting in:

$$k_{ct} = GJ_c / L_{ce} \quad (8)$$

where GJ_c represents the torsional rigidity of the cap beam. For the concrete cap beams in this study, the recommendation of Priestley et al. (1996) to use 0.05 J (where J is the polar moment of inertia) for cracked sections was used to determine J_c.

The resulting total stiffness value for the typical lateral load configuration, k_{lat}, and stiffness value related to the cap and exterior girder contribution, k_{et+ct}, are:

$$k_{lat} = (k_{et}k_{ct}) / (k_{et} + k_{ct}) + k_{it} \quad (9)$$

$$k_{et+ct} = (k_{et}k_{ct}) / (k_{et} + k_{ct}) \quad (10)$$

and the lateral load distribution factors are:

$$DF_{int} = k_{lat} / (k_{lat} + k_{et+ct}) \quad (11)$$

$$DF_{ext} = k_{et+ct} / (k_{lat} + k_{et+ct}) = 1 – DF_{int} \quad (12)$$

These distribution factors can be used to estimate the fractional load distribution of the column overstrength moment to the interior and exterior girders, respectively.

Grillage and FEA Models

Grillage model analyses (GMAs) were conducted for each of the experimental studies considered in this work. The results from these GMAs are used for comparison with the SSM approach and the experimental results from each test unit. Fig. 5 shows a schematic of the GMA used for the ITB model (Snyder et al. 2011). Member section properties for the line elements in this GMA are calculated using composite section properties, incorporating cracked or uncracked concrete properties similar to the approach described for the SSM calculations in the preceding section. Nonlinear springs are also incorporated in GMA, located in the plastic hinge regions of the reinforced concrete column. The spring behavior is defined by using appropriate analytical methods to determine moment-rotation behavior for the spring based on the predicted moment-curvature for the column section in the plastic hinge region (see Priestley et al. 1996, for example). Similar GMAs have been conducted for each of the test units used in this study. Information on the grillage model for the PBT study can be found in Holombo et al. (2000) and for the SPC study in Wassef et al. (2004).

All the GMAs included the contributions of the slab and diaphragm members to provide limited transverse continuity between girders. The deck and diaphragm contribution is at times observed to play a noticeable role in the load distribution among girders. The deck contribution in particular affects load distribution in the structures likely to experience degradation in the connections, since the connection deterioration produces variation in stiffness among the girders. When a stiffness difference exists among the girders, the deck contribution appears to play a larger role in transferring load from girder to girder. In the ITB study, a detailed FEA model was also developed in parallel with the GMA. Detailed information on this FEA work can be found in Theimann (2009). The FEA analysis results are not identical to the GMA results, but

they confirm that inclusion of deck and diaphragm elements can affect the lateral load distribution results.

The stiffness-based SSM approach, described in the preceding section, is not well-suited to include the contribution of transverse elements such as deck and diaphragm. This limitation is a result of using stiffness values based on beam elements that are representative of individual, isolated girders. However, as will be seen in the results presented later, the SSM approach can still be a very serviceable option in predicting load distribution.

Summary of Large-Scale Tests

All the studies in this work included large-scale test units intended to examine and quantify system performance. All the test units modeled prototype structures utilizing an integral bent cap and a single reinforced concrete column. The prototype structures, presented in Fig. 1, were modeled experimentally to examine and quantify performance of the PBT, ITB, and SPC systems. Fig. 6 shows the configuration for the ITB test unit. Detailed information on the test configuration and experimental results can be found in Holombo et al. (2000) for the PBT test, Sritharan et al. (2005) for the SPC tests, and Snyder et al. (2011) for the ITB test.

PBT Test Unit

The test unit for the PBT study was constructed as a 40-percent scale representation of a prototype bridge utilizing precast, prestressed concrete bulb-tee girders. The test unit modeled the prototype bridge from midspan to midspan of the two spans adjacent to the center bent. The test unit included the reinforced concrete column, the post-tensioned concrete cap beam,

and portions of the girders extending across the cap beam to a scaled distance equivalent to the midspan of the prototype center spans. The load-displacement for the horizontal seismic loading is shown in Fig. 7a. The test unit was observed to exhibit very good seismic behavior, retaining strength up to a lateral displacement ductility $\mu_\Delta = 8$.

SPC Test Units

Test units SPC1 and SPC2 were constructed for the NCHRP study. Both test units were similar, except SPC2 was designed and constructed with a reduced superstructure depth. The test units were built in an inverted configuration to simplify the laboratory setup and loading. These test units were one-third-scale representations of the region surrounding the center bent of a prototype bridge consisting of steel I-girders and a steel box-shaped cap beam. The test units included a reinforced-concrete column, steel box beam pier cap, and steel girders extending to the midspan of the spans adjacent to the column. To account for the dead load in the inverted position, a vertical load was applied to the reinforced concrete column at its top (in the test orientation).

Figs. 7b and 7c provide the load-displacement hysteresis behavior for SPC1 and SPC2 when subjected to simulated horizontal seismic loading. The test units were both observed to perform well. The superstructure in SPC1 exhibited elastic response throughout the duration of the test, and a plastic hinge was successfully formed in the column. The horizontal load test showed the structure to retain full strength up to target ductility, $\mu_\Delta = 4$, and reduced strength with no stability failure up to ductility $\mu_\Delta = 6$. Longitudinal bar buckling and subsequent fracture just below the cap beam was observed to be the primary failure mechanism. SPC2 also

exhibited good overall seismic behavior. Stresses in the superstructure were observed to remain elastic throughout the horizontal test, and the structure also retained close to full strength up to ductility 4, with significant strength, although reduced, at ductility 6. The primary failure mechanism in SPC2 was the fracture of mechanical anchorage of the column longitudinal bars in the bridge deck near the cap beam.

Both SPC1 and SPC2 were subjected to service-level loading prior to the seismic loading. In these service level tests, vertical load and horizontal load were applied separately. Data from these tests, including girder strains and girder reactions, have been used to compile the results presented in the distribution comparisons later in this paper.

ITB Test Unit

The half-scale test unit for the ITB study modeled a portion of the reinforced concrete column, the cast-in-place concrete cap beam, and the central portion of the five precast concrete I-shaped girders on both sides of the cap beam. Two different integral connection details between the girders and cap beam were utilized, one on one side of the cap beam and the other on the opposite side. The first detail implemented a design that has already been used by Caltrans, referred to as the “as-built” connection. The connection detail on the other side of the cap beam was similar but incorporated an unstressed post-tensioning tendon to provide continuity for the positive-moment tension reinforcement through the connection. The tendon passed through the bottom flange of the girder and the cap beam corbel and then terminated on the far side of the cap beam. This connection is referred to as the “improved” connection. Although data was gathered from both the as-built and improved details, the data used in the

distribution analysis presented in this paper are from only the improved connection portion of the test unit. The as-built data has been omitted since the improved connection configuration is likely more representative of future bridges based on this concept.

Fig. 7d shows the load-displacement hysteresis for the test unit when subjected to simulated horizontal seismic loading. The system was observed to perform very well. The superstructure provided sufficient strength to successfully form plastic hinges in the column, and the structure maintained strength up to displacement ductility $\mu_\Delta = 8$ with only minor strength loss at ductility $\mu_\Delta = 10$. The load-displacement hysteresis and high displacement ductility attained by the test unit show that the girder-to-cap connection performed well, remaining elastic while allowing full development of the column plastic hinges.

Comparison of Analytical and Experimental Load Distributions

Vertical Load

Using the approach described in the "Analytical Approaches" section, SSMs have been developed for each of the test units to investigate the distribution of the moment in the girders due to the vertical load. In addition, results from GMAs of each of the test units also have been used to look at the distribution of moment due to vertical load. Finally, the experimental results from each of the test units, summarized above, have been incorporated to further validate the analytical models.

Table 1 provides a compilation of the distribution of moment due to vertical load in the SPC and ITB test units, including experimental data, grillage model predictions, and SSM predictions. (The PBT test unit was not included in this comparison since corresponding experimental data was not available.) Also included in this table are the distribution ratios from AASHTO (2010), representing the current design recommendations. The design ratios included in this table are determined using the AASHTO specifications for live load distribution factors, even though these factors are not directly comparable to the results from the vertical SSM analysis as mentioned previously.

The ratios for the experimental and analytical distributions reported in this table are determined on the basis of total load in all girders. Hence, for a five-girder structure, if each of the five girders would carry the same amount of load, the resulting ratio would be 0.20 for the center girder, 0.20 for each of the two intermediate girders, and 0.20 for each of the two exterior girders. The “difference” listed for each model in the table is the percentage difference between the analytical prediction and the experimental result.

The predictions in Table 1 from the design recommendations for live load distribution, the grillage analyses, and the SSM analyses all compare favorably with the measured experimental results. This favorable comparison is notable, since the design recommendation values are actually intended for live load distribution rather than for vertical load transfer during seismic loading. The values determined by current design recommendations for live load distribution vary a maximum of 5% from the experimental values. The SSM predictions are similar, with a maximum difference of 6.2%. The largest discrepancy occurs in the grillage prediction for the

ITB model, with a difference of approximately 12% in the predicted and experimental values for the intermediate and exterior girders.

Horizontal Load

For the lateral load SSMs, the approach presented in the "SSM for Lateral Load" section has been followed, except the model is altered slightly for the five-girder ITB structure. Because of the direct connection of the column, center girder, and cap beam, the general SSM approach is found to overestimate the load distribution to the center girder. Therefore, the predicted distribution of the load to the center girder is determined by comparing only the girder stiffness values and not the overall system stiffness values (resulting in a distribution of 0.20 to the center girder). Once the center girder distribution is predicted in this way, the SSM as presented is used to predict the intermediate and exterior girder distributions.

Results from the grillage model analyses of each of the test units have also been incorporated to predict the distribution of the lateral load moment. Experimental results from each of the test units are then compared to both the SSM and grillage analytical predictions along with the current design recommendations for lateral load distribution. Since none of the test units were subjected to horizontal-load-only conditions, the horizontal-load-only experimental values have been determined by removing the vertical load contribution from the recorded strain or load data. This process has been accomplished by carefully identifying the zero-horizontal-load instances during each cycle of the horizontal load tests. The measured strains and displacements at these instances have been identified as vertical-load-only data. Subsequently, the vertical-load-only data has been found to be acceptably consistent throughout the lateral

load test. Thus, for the portions of the test where lateral load was present, the vertical-load-only data is used to bias the overall data and provide the horizontal-load-only data.

Table 2 lists the experimental values, analytical predictions, and current design recommendations for seismic lateral load only. The reported experimental distribution values have been established at the first peak displacements by comparing the strain increase in each girder as the lateral load was increased from zero to the load corresponding to the target displacement during each displacement half cycle.

As with the information in Table 1, the data in this table are reported on the basis of load ratio in each of the individual girders compared to the total load experienced in all girders. The first observation regarding these numbers is the striking dissimilarity of the design ratio numbers to the actual experimental values. Current design recommendations allow lateral load distribution among only the center and intermediate girders of the ITB structure, which is the only five-girder structure included in this investigation. However, an examination of the experimental data reveals that 15.8% of the lateral load was carried by each of the exterior girders, i.e., the two exterior girders together carried almost 32% of the total lateral load moment. The strains used to determine these distributions were measured directly above the connection interface and at a location approximately 450 mm along the girder from the connection interface. Caltrans' current recommendations would not allow distribution of the load to the exterior girders until reaching a distance of approximately 990 mm from the connection (the distance corresponding to d_g in Fig. 2 presented earlier). Hence, the measured distributions clearly show the distribution is happening sooner than the current recommended practice.

The data from the four-girder structures (PBT, SPC 1, and SPC 2) reveal even less correlation with the current design recommendations. For these structures, current design guidelines allow no distribution of lateral load to the exterior girders in the connection region; however, the experimental results show that 30%, 33%, and 34% of the total lateral load moment is distributed to the exterior girders in the PBT, SPC 1, and SPC 2 test units, respectively. The results indicate that current design recommendations are overly conservative in confining the lateral load only to the interior girders adjacent to the column.

While the analytical predictions for each of the four structures considered have some discrepancy, the results from the SSMs and GMAs from all four of the structures compare better with the experimental results than the current design recommendations do. Looking at the GMAs, the maximum difference between the predicted ratios and the experimental ratios is 0.03, whereas the design recommendations consistently differ from the experimental ratios by 0.15 or more. The SSMs also provide much better comparisons to the experimental results than current design predictions, with a maximum ratio discrepancy of about 0.04. The experimental results validate the predictions of both the GMAs and SSMs, showing that large portions of the lateral load are indeed distributed beyond the girders immediately adjacent to the column.

Lateral Load Distribution at Various Load Levels

Data gathered from the SPC2 and ITB tests are helpful in investigating whether the lateral load distribution occurs consistently at low and high seismic load levels. Fig. 8 shows the experimental load distribution for SPC2 for the peak conditions throughout the test, beginning at service load levels and continuing through several cycles of plastic deformation. The girder

load distribution to the exterior girders is seen here to begin almost immediately, at the first recorded load level. The load level at this point of the test is only $0.25F_y$, with F_y representing the lateral yield of the test unit. The exterior girders even at this early stage are carrying approximately 30 percent of the lateral load. Observed flexural cracking of the concrete across the entirety of the deck width prior to the $1.0F_y$ load level also indicates the engagement of all the girders in carrying the lateral load. The distribution to the exterior girders remains quite consistent throughout the duration of the load test. Thus, the SSM and GMA predictions for the superstructure are useful not only at high levels of seismic loading but also at service load levels.

Fig. 9 provides the load distributions at various load levels for the ITB test unit. These results show significant and relatively consistent distribution to all girders. The exterior girders are shown, at the very first peak load recorded, to individually carry 15 percent (30 percent combined) of the total lateral load. These results concur with the results from SPC2. Although there is a bit of irregularity in the distribution for the low loads, likely related to initial cracking and softening, significant distribution is observed at the early stages of loading followed by more uniform distribution for all of the higher peak conditions.

Recommended Model for Lateral Load Distribution

The work presented here shows the SSM is useful for predicting lateral load distribution for bridges with integral girder-to-cap connections. The SSM can provide a simple approach for determining more realistic lateral load distribution than the current design recommendations.

Based on the SSM results presented previously, a suitable approach is to use the SSM prediction for all girders along with an appropriate variability margin. If α is introduced as a variability factor, and DF_{SSM} is defined as the girder distribution factors determined from Eqs. 11 and 12 as appropriate, the recommended distribution factor, DF_{recom}, can be defined as:

$$DF_{recom} = \alpha \, DF_{SSM} \tag{13}$$

The variability factor, α, is introduced to provide a safety margin since the simple model is not intended to be an exact representation of all the complexities of the real structure. Trial-and-error reveals that a value of 1.2 provides good results for the four structures in this study; similar studies could be used to further refine this variability factor. Using $\alpha = 1.2$ and the interior fractional distribution values from Table 2 for each test unit, the recommended distributions for the interior girders in this study are 0.37, 0.44, 0.42, and 0.29, respectively, for the PBT, SPC1, SPC2, and ITB test units. The ratios of these recommended distributions to the measured experimental distributions range from 1.10 for the PTB test unit to 1.34 for the SPC1 test unit. The recommended distributions are shown graphically in Fig. 10 (“Proposed”) along with the current AASHTO/Caltrans approach (“Current”) and compared with the experimental, GMA, and SSM predictions. Examining the data from the interior girders in the PBT test unit, the ratio of the current recommendation to the experimental distribution is 1.50. However, the ratio of the proposed recommendation to the experimental distribution is 1.10. Thus, when compared with current design recommendations, the SSM prediction for the PBT structure compares 40% more favorably with the experimental results. The improvements of the SSM

model in distribution prediction for the SPC1, SPC2, and ITB structures are 17%, 22%, and 19%, respectively.

Conclusions

This study focused on the development of simple stiffness models (SSMs) to predict seismic load distribution between girders in integral bridge superstructures. The conclusions drawn from this study are presented below:

1. Current practice and recommendations related to vertical distribution of dead load and vehicle live load are appropriate. Under high seismic horizontal displacements, the experimental girder strain values due to vertical load increase, but the vertical load distribution between girders remains relatively constant. Vertical load distributions determined using techniques such as the vertical simple stiffness model (SSM) and grillage model analysis (GMA) are shown to match well with current recommendations and experimental results.
2. Current practice and recommendations limit the distribution of column seismic overstrength moment—expected under horizontal seismic action longitudinally along the bridge—to the girders in the superstructure immediately adjacent to the column. Observed load distributions from large-scale tests confirm the girders that are not adjacent to the column consistently resist a significant amount of the column moment.
3. Load predictions determined using the lateral load SSM compare favorably with more complex GMA techniques. The ratios of GMA interior girder distribution to SSM interior

girder distribution are 1.10, 0.98, 0.99, and 0.89, for the PBT, SPC 1, SPC 2, and ITB structures, respectively. The largest difference between GMA and SSM predictions is for the ITB structure (a difference of 11.3%), and in this instance the SSM prediction matches the experimental distribution almost exactly while the more complex GMA technique provides a poorer prediction.

4. The analytical predictions of lateral load distribution to the interior girders based on the SSM model average a difference of 5.0% from the experimental distribution values, with a maximum difference of 9.8%. The average percentage difference of the GMA predictions from the experimental values is 5.9%, with a maximum difference of 12.7%.
5. At very low levels of lateral load (as low as 0.25 F_y, with F_y representing column yield due to lateral load), the test units consistently show at least 15% of the lateral load being distributed to the exterior girders. This distribution remains almost constant all the way to the maximum displacement ductility levels (as high as $\mu_D = 10.0$) experienced by each test unit.
6. Current design recommendations overestimate the lateral load distribution to the girders adjacent to the column by as much as 60%. As described in Conclusion 4, the SSM approach provides significant improvement in the distribution predictions without implementing a more complex analytical approach. When using the SSM approach, a multiplier of 1.2 is recommended over the calculated distribution factor, based on the results from the four structures in this study. The design girder moment determined using the SSM approach is then expected to be 10% to 20% higher than the measured moment, a marked improvement over current recommendations. Improved distribution

predictions will likely lead to shallower girders due to reduced demand in the connection region.

Acknowledgements

The large-scale tests which provided the data for this paper were made possible through funding from the California Department of Transportation (Caltrans) for the PBT and ITB units and the National Cooperative Highway Research Program (NCHRP) for the SPC units. The authors also wish to thank Jay Holombo, of T.Y. Lin International Group, Robert Abendroth, of Iowa State University (ISU), and Ryan Staudt, former graduate student of ISU, for their contributions to this study.

References

AASHTO Guide Specifications for LRFD Seismic Bridge Design. (2009). American Association of State Highway and Transportation Officials (AASHTO), Washington, D. C.

AASHTO LRFD Bridge Design Specifications, 5th Edition. (2010). AASHTO, Washington, D. C.

Barr, P., Eberhard, M. O., and Stanton, J. (2001). "Live-load distribution factors in prestressed concrete girder bridges." *Journal of Bridge Engineering,* 6(5), 298-306.

Bridge Design Aids. (1995). California Department of Transportation, Sacramento, CA.

Cai, C. S. (2005). "Discussion on AASHTO LRFD Load Distribution Factors for Slab-on-Girder Bridges." *Practice Periodical on Structural Design and Construction,* 10(3), 171-176.

California Amendments to AASHTO LRFD Bridge Design Specifications – Fourth Edition. (2011). California Department of Transportation, Sacramento, CA, 4-34A.

"Concrete box girder live load distribution by Lanell for special loads." (1988). *Bridge Memo to Designers,* California Department of Transportation, Sacramento, CA.

Holombo, J. M., Priestley, J. N., Seible, F. (2000). "Continuity of Precast Prestressed Spliced-Girder Bridges Under Seismic Loads." *PCI Journal,* 45(2), 40-63.

Kim, S. and Nowak, A. S. (1997). "Load distribution and impact factors for I-girder bridges." *Journal of Bridge Engineering,* 2(3), 97-104.

Mabsout, M. E., Tarhini, K. M., Frederick, G. R., and Kesserwan, A. (1999). "Effect of multilanes on wheel load distribution in steel girder bridges." *Journal of Bridge Engineering,* 4(2), 88-106.

Maruri, R. and Petro, S. (2005). "Integral Abutments and Jointless Bridges (IAJB) 2004 Survey Summary." *Proc., 2005 Integral Abutment and Jointless Bridges Conference (IAJB 2005),* Federal Highway Administration (FHWA), Washington, D. C., 12-29.

Mertz, D. (2007). *NCHRP Report 592: Simplified Live Load Distribution Factor Eq.s,* Transportation Research Board (TRB), Washington, D. C.

Priestley, M. J. N., Seible, F., and Calvi, G. M. (1996). *Seismic Design and Retrofit of Bridges,* John Wiley and Sons, Inc., New York, NY.

Seismic Design Criteria, Version 1.4. (2006). California Department of Transportation, Sacramento, CA.

Snyder, R. M. (2010). “Seismic performance of an I-girder to inverted-T bent cap bridge connection.” M. S. Thesis, Iowa State University (ISU), Ames, IA.

Snyder, R. M., Vander Werff, J., Theimann, Z. J., Sritharan, S., and Holombo, J. (2011). *Seismic Performance of an I-Girder to Inverted-T Bent Cap Connection, Final Report,* Caltrans, Sacramento, CA, and ISU, Ames, IA.

Sritharan, S., Vander Werff, J., Abendroth, R. E., Wassef, W. G., Greimann, L. F. (2005). “Seismic Behavior of a Concrete/Steel Integral Bridge Pier System.” *Journal of Structural Engineering,* 131(7), 1083-1094.

Theimann, Z. J. (2009). “3-D finite element analysis of the girder-to-cap beam connection on an inverted-tee cap beam designed for seismic loadings.” M. S. Thesis, ISU, Ames, IA.

Vander Werff, J. R. (2002). “Steel girder-concrete column integral bridges for seismic regions.” M. S. Thesis, ISU, Ames, IA.

Wassef, W. G., Davis, D., Sritharan, S., Vander Werff, J. R., Abendroth, R. E., Redmond, J., and Greimann, L. F. (2004). *NCHRP Report 527: Integral Steel Box-Beam Pier Caps,* TRB, Washington, D. C.

Zokaie, T., Osterkamp, T. A., and Imbsen, R. A. (1991). *NCHRP Report 12-26/1: Distribution of Wheel Load on Highway Bridges,* TRB, Washington, D. C.

Table 1. Vertical load distribution comparison

Parameters	SPC 1		SPC 2		ITB		
	Interior	Exterior	Interior	Exterior	Center	Intermediate	Exterior
Experimental Ratio	0.258	0.242	0.268	0.233	0.208	0.195	0.2
Design Ratio	0.271	0.229	0.271	0.229	0.203	0.203	0.196
Design Difference	4.7%	-5.0%	1.1%	-1.3%	-2.4%	4.1%	-2.0%
Grillage Ratio	0.275	0.225	0.273	0.228	0.211	0.219	0.176
Grillage Difference	6.5%	-6.9%	1.9%	-2.2%	1.4%	12.3%	-12.0%
SSM Ratio	0.258	0.242	0.253	0.247	0.208	0.2	0.196
SSM Difference	0.0%	0.0%	-5.4%	6.2%	0.0%	2.6%	-2.0%

Table 2. Lateral load distribution comparison

Parameters	PBT		SPC 1		SPC 2		ITB		
	Interior	Exterior	Interior	Exterior	Interior	Exterior	Center	Interm.	Exterior
Experimental Ratio	0.334	0.166	0.333	0.167	0.350	0.150	0.205	0.239	0.158
Design Ratio	0.5	0	0.5	0	0.5	0	0.333	0.333	0
Design Difference	49.9%	-100.0%	52.1%	-100.0%	42.9%	-100.0%	62.4%	39.3%	-100.0%
GMA Ratio	0.344	0.156	0.360	0.140	0.349	0.151	0.228	0.212	0.174
GMA Difference	2.9%	-6.4%	7.5%	-19.3%	-0.003%	0.01%	2.3%	-12.7%	9.2%
SSM Ratio	0.305	0.195	0.369	0.131	0.353	0.147	0.200	0.239	0.158
SSM Difference	-9.5%	17.1%	9.8%	-23.7%	0.01%	-1.7%	-2.4%	0%	0%

Fig. 1a

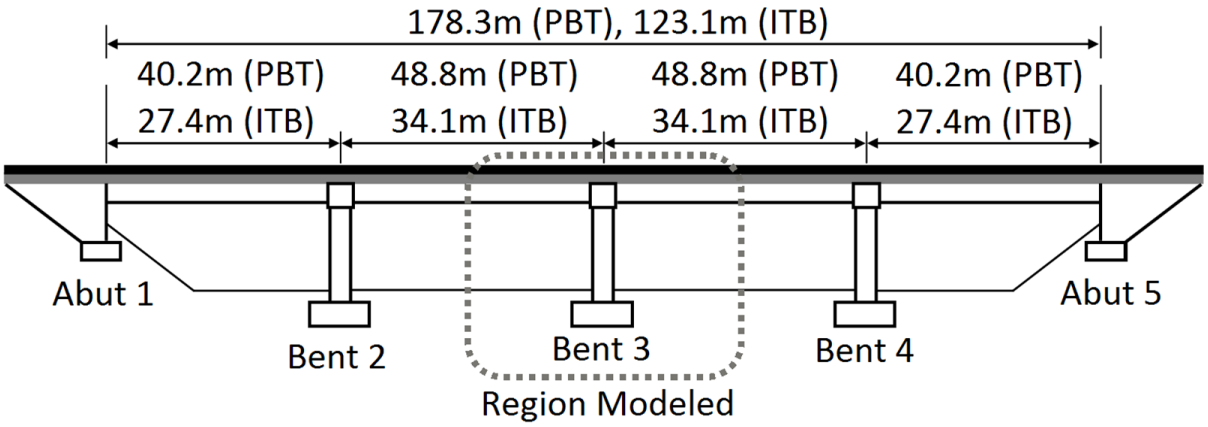
178.3m (PBT), 123.1m (ITB)
40.2m (PBT)
27.4m (ITB)
48.8m (PBT)
34.1m (ITB)
48.8m (PBT)
34.1m (ITB)
40.2m (PBT)
27.4m (ITB)
Abut 1
Bent 2
Bent 3
Bent 4
Abut 5
Region Modeled

Fig. 1b

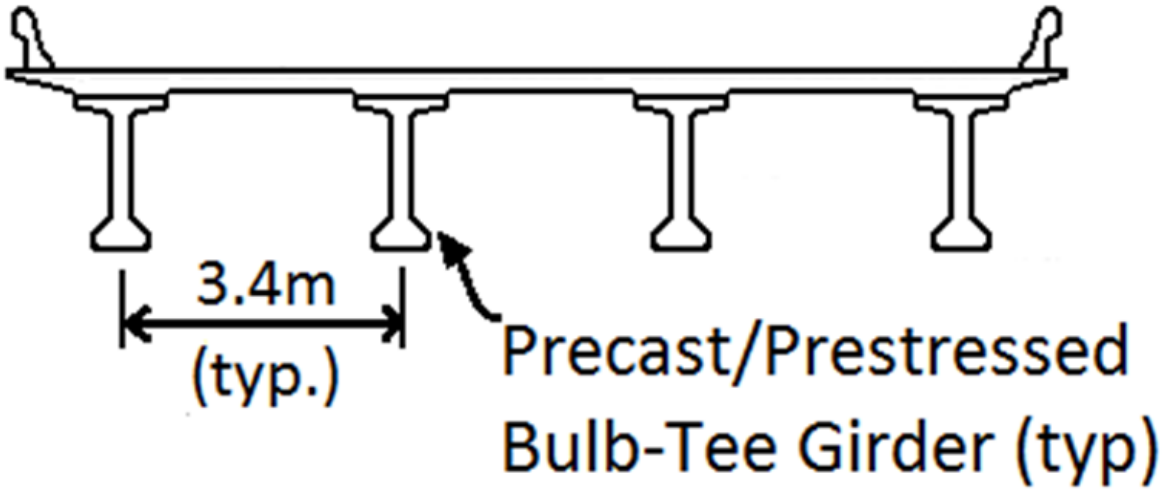
3.4m
(typ.)
Precast/Prestressed
Bulb-Tee Girder (typ)

Fig. 1c

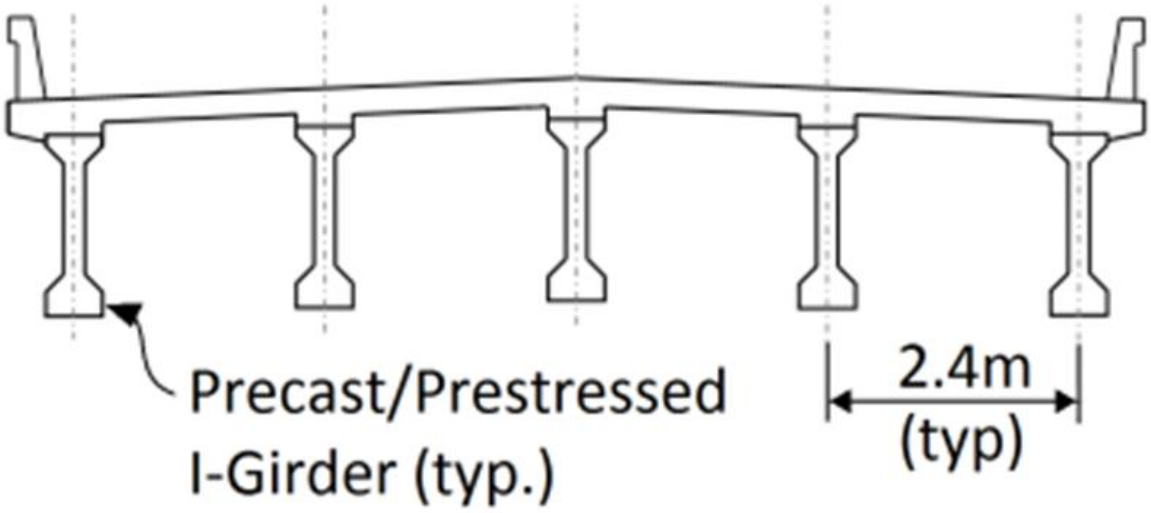
Precast/Prestressed
I-Girder (typ.)
2.4m
(typ)

Fig. 1d

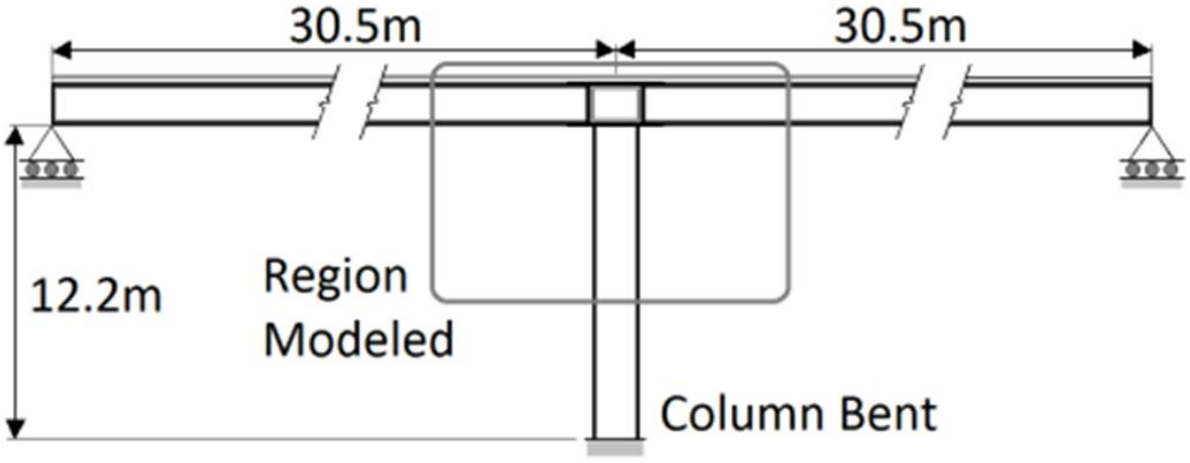
30.5m
30.5m
12.2m
Region
Modeled
Column Bent

Fig. 1e

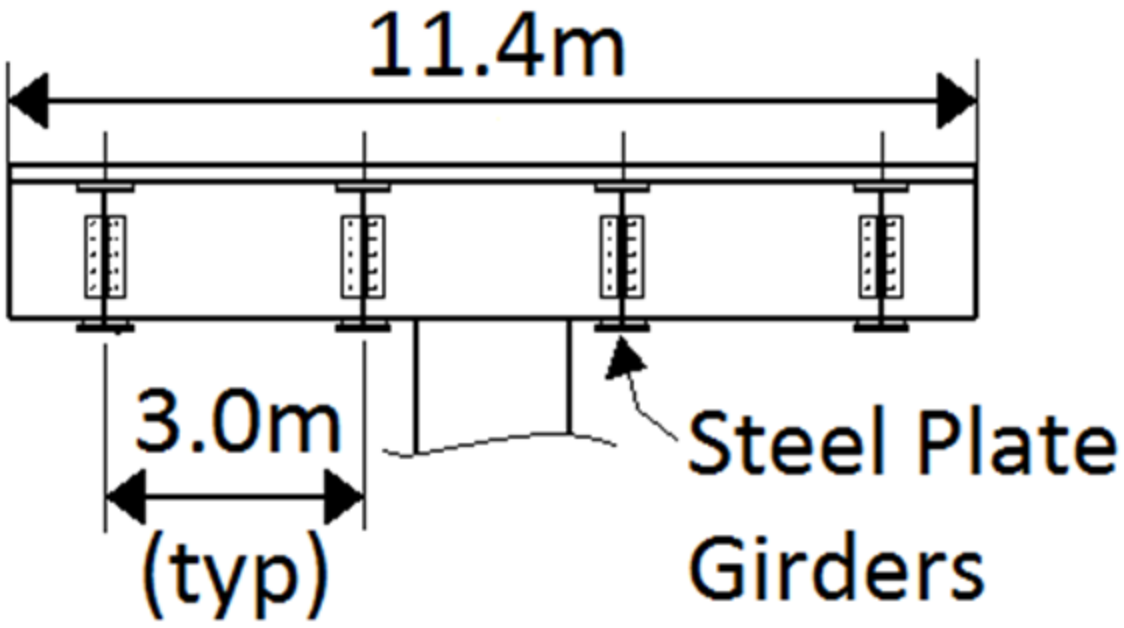
11.4m
3.0m
(typ)
Steel Plate
Girders

Fig. 2

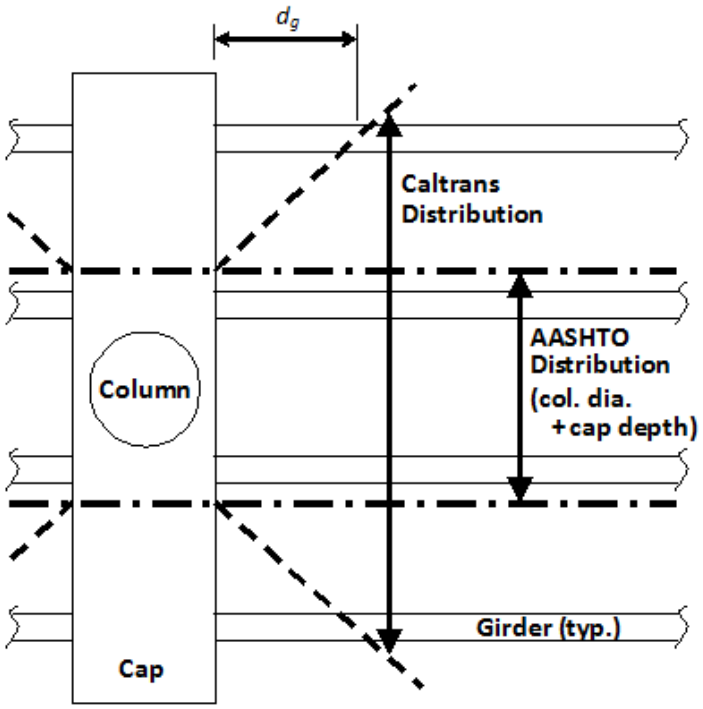
d_g
Caltrans
Distribution
AASHTO
Distribution
(col. dia.
+cap depth)
Column
Girder (typ.)
Cap

Fig. 3a

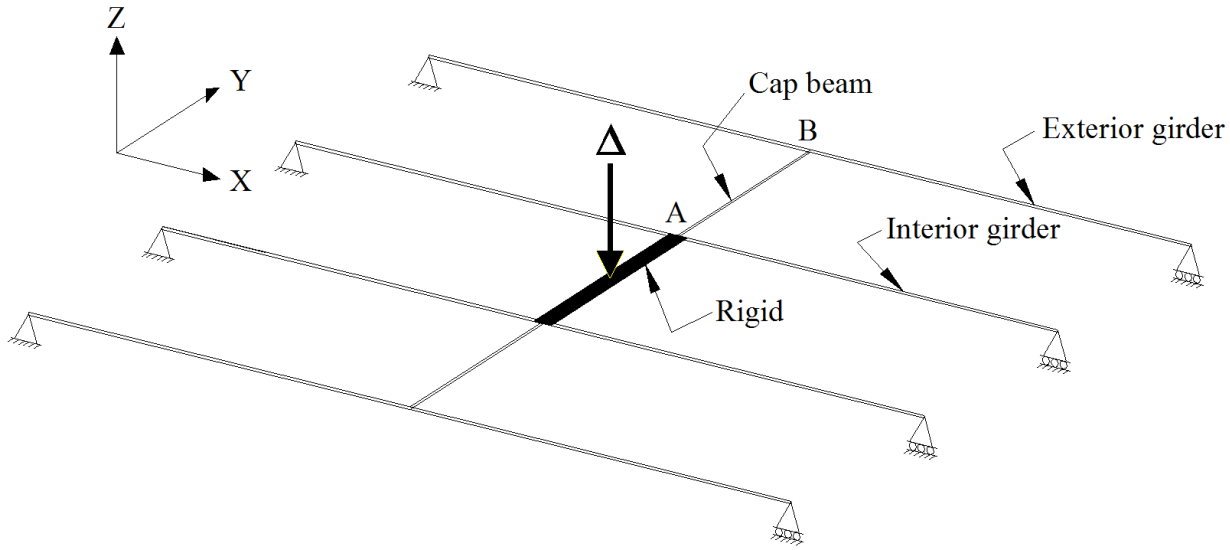
Z
Y
X
Δ
Cap beam
B
Exterior girder
A
Interior girder
Rigid

Fig. 3b

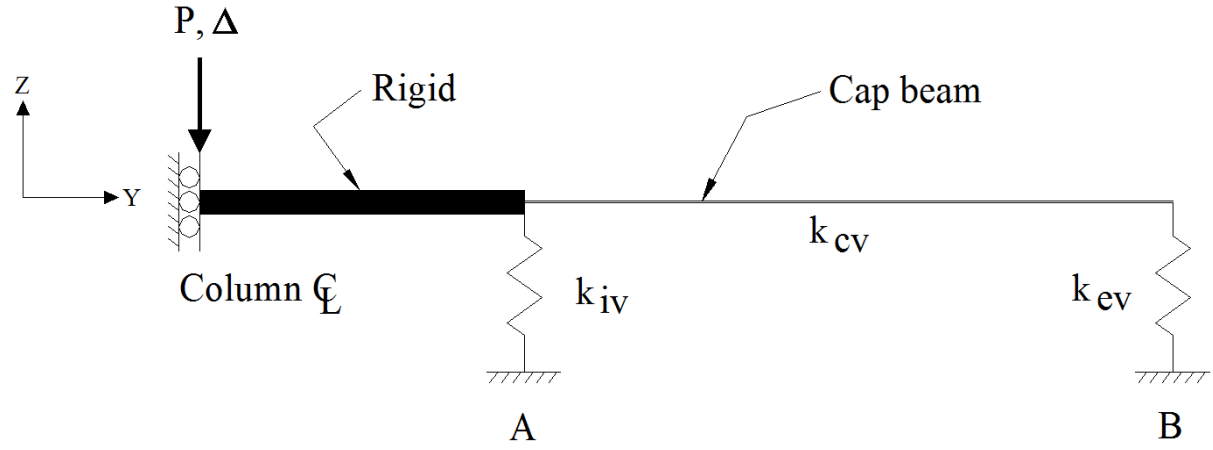
P, Δ
Z
Y
Rigid
Cap beam
k cv
Column ℄
k iv
k ev
A
B

Fig. 3c

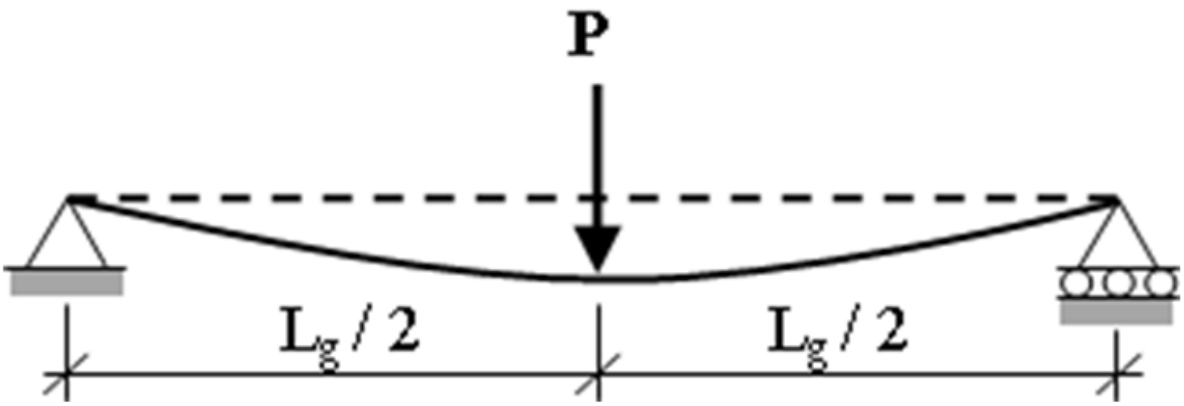

Fig. 3d

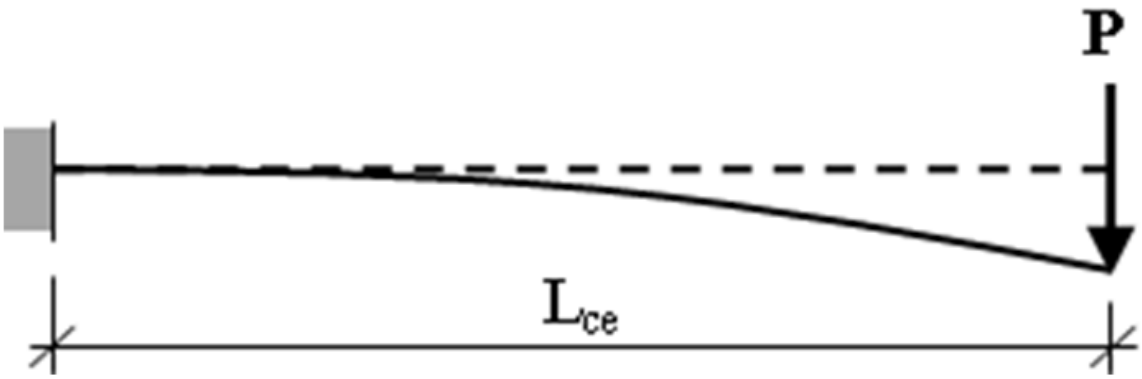

Fig. 4a

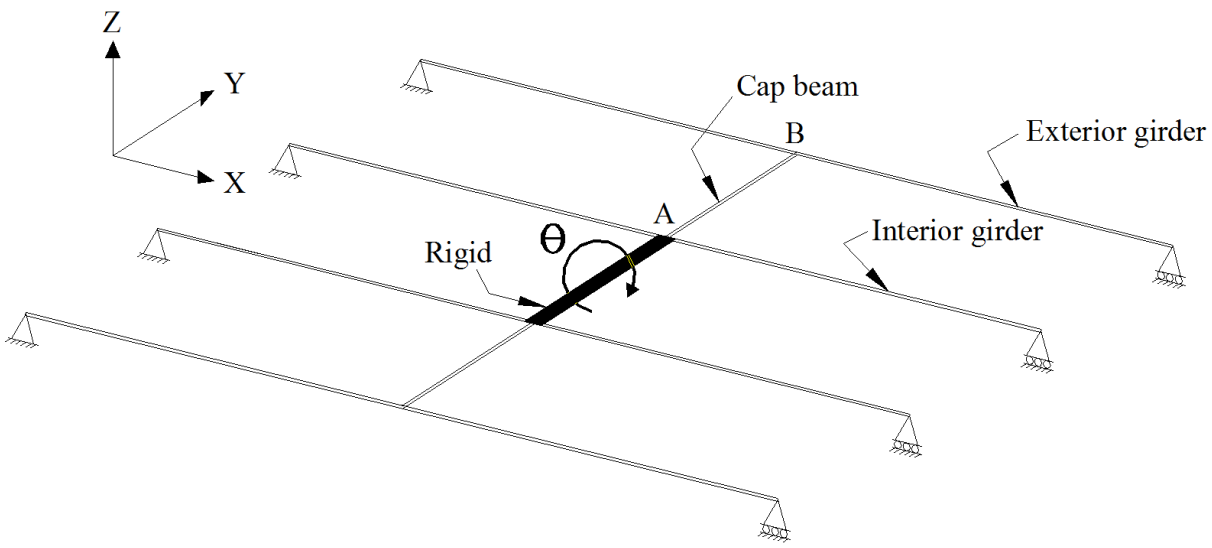
Z
Y
X
Cap beam
B
Exterior girder
A
Interior girder
Rigid
θ

Fig. 4b

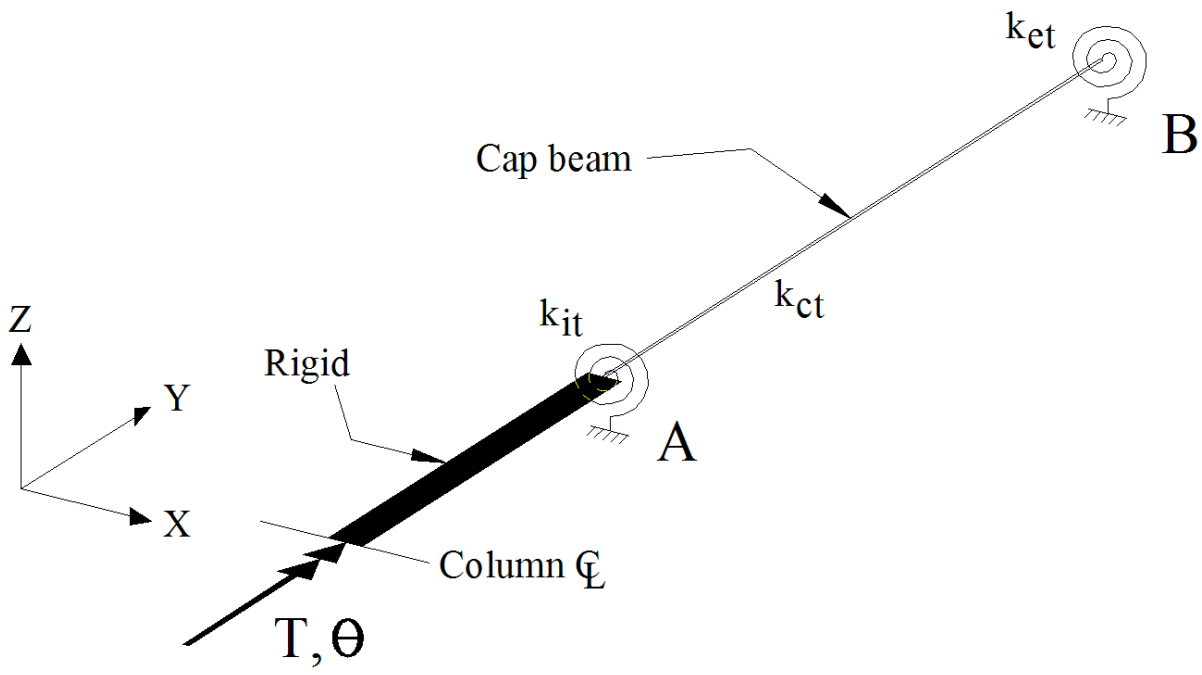
k_{et}
B
Cap beam
k_{ct}
k_{it}
Z
Rigid
Y
A
X
Column ℄
T, θ

Fig. 4c

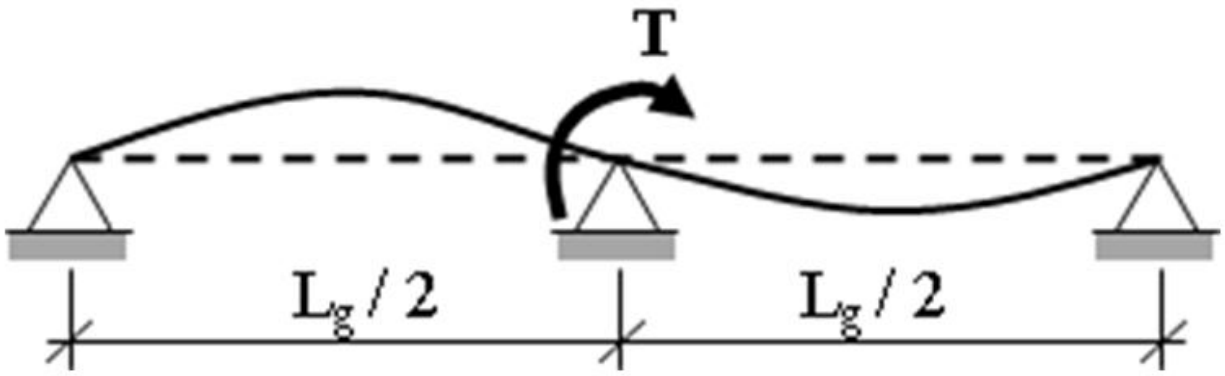

Fig. 4d

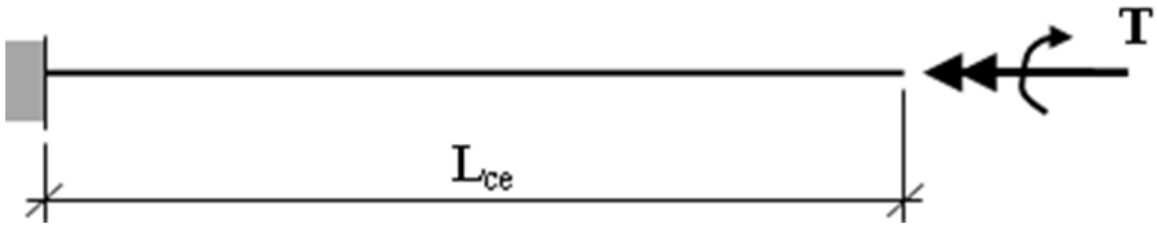

Fig. 5

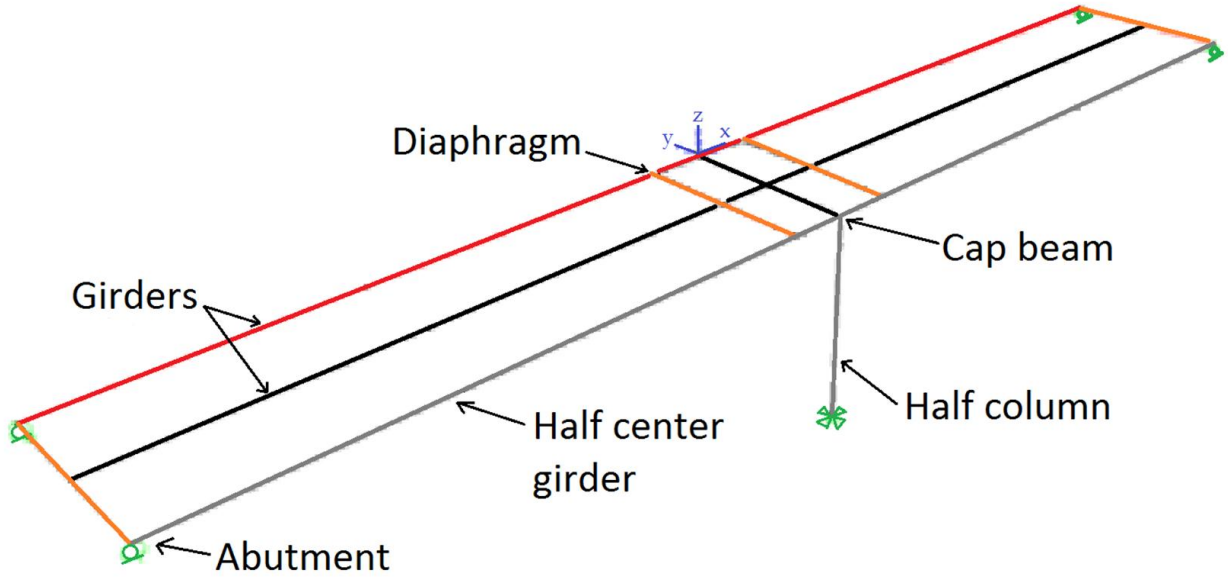

Fig. 6

Fig. 7a

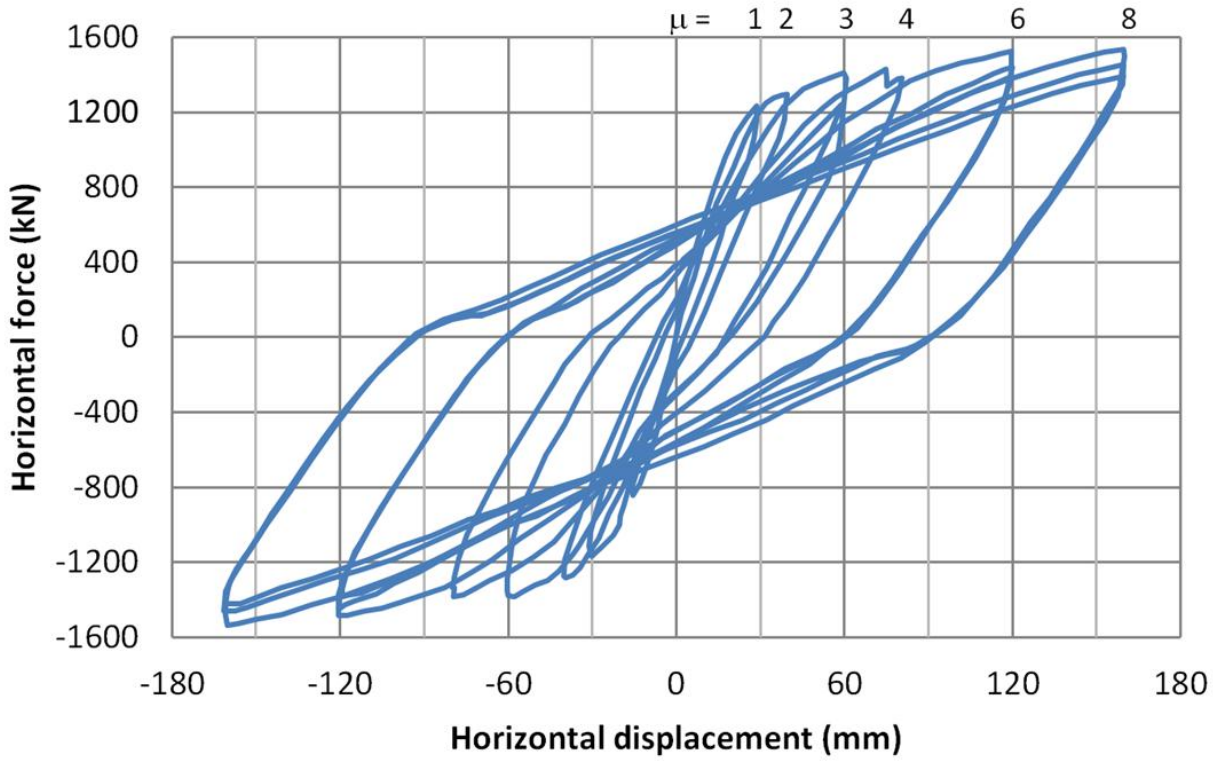
μ = 1 2 3 4 6 8
1600
1200
800
400
0
-400
-800
-1200
-1600
Horizontal force (kN)
-180
-120
-60
0
60
120
180
Horizontal displacement (mm)

Fig. 7b

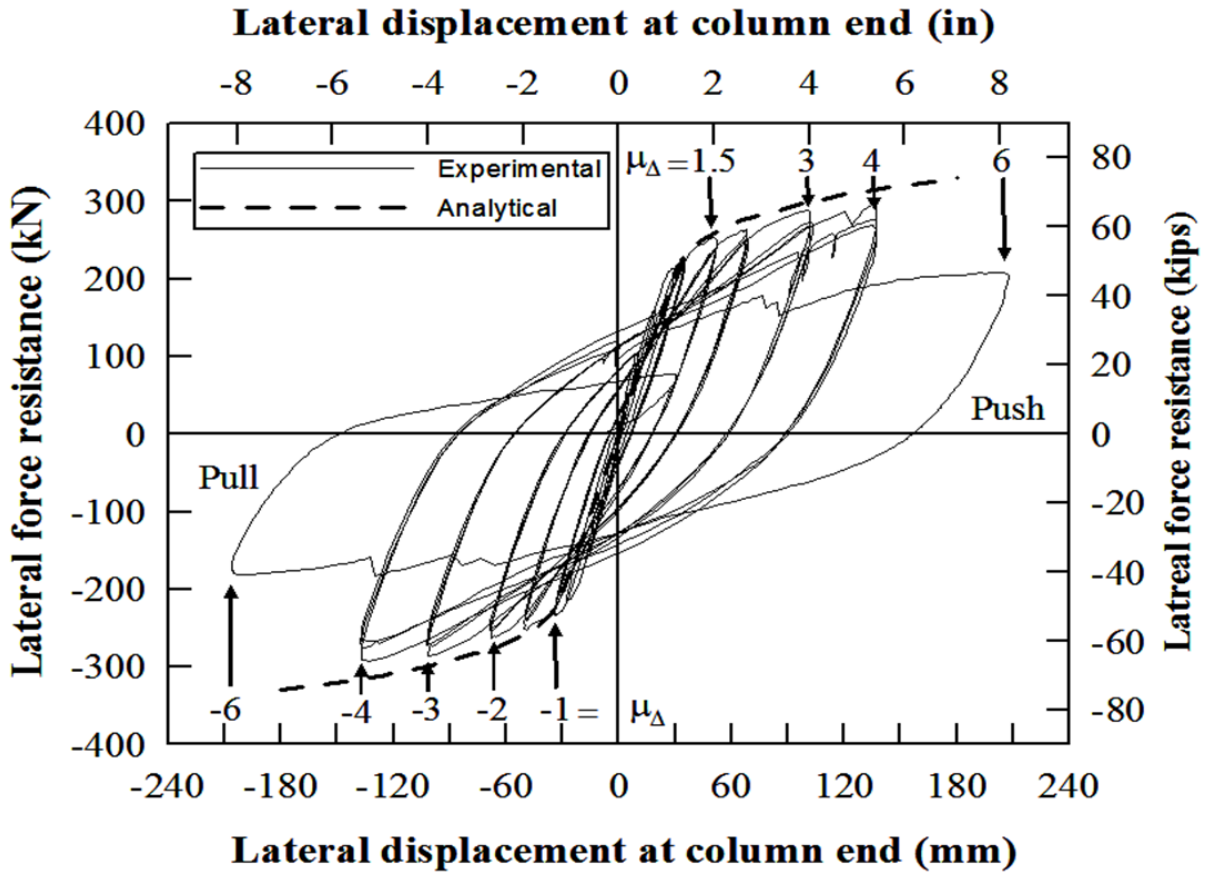
Lateral displacement at column end (in)
-8 -6 -4 -2 0 2 4 6 8
Experimental
Analytical
μΔ=1.5 3 4 6
Push
Pull
-6 -4 -3 -2 -1= μΔ
Lateral force resistance (kN)
400 300 200 100 0 -100 -200 -300 -400
Latreal force resistance (kips)
80 60 40 20 0 -20 -40 -60 -80
-240 -180 -120 -60 0 60 120 180 240
Lateral displacement at column end (mm)

Fig. 7c

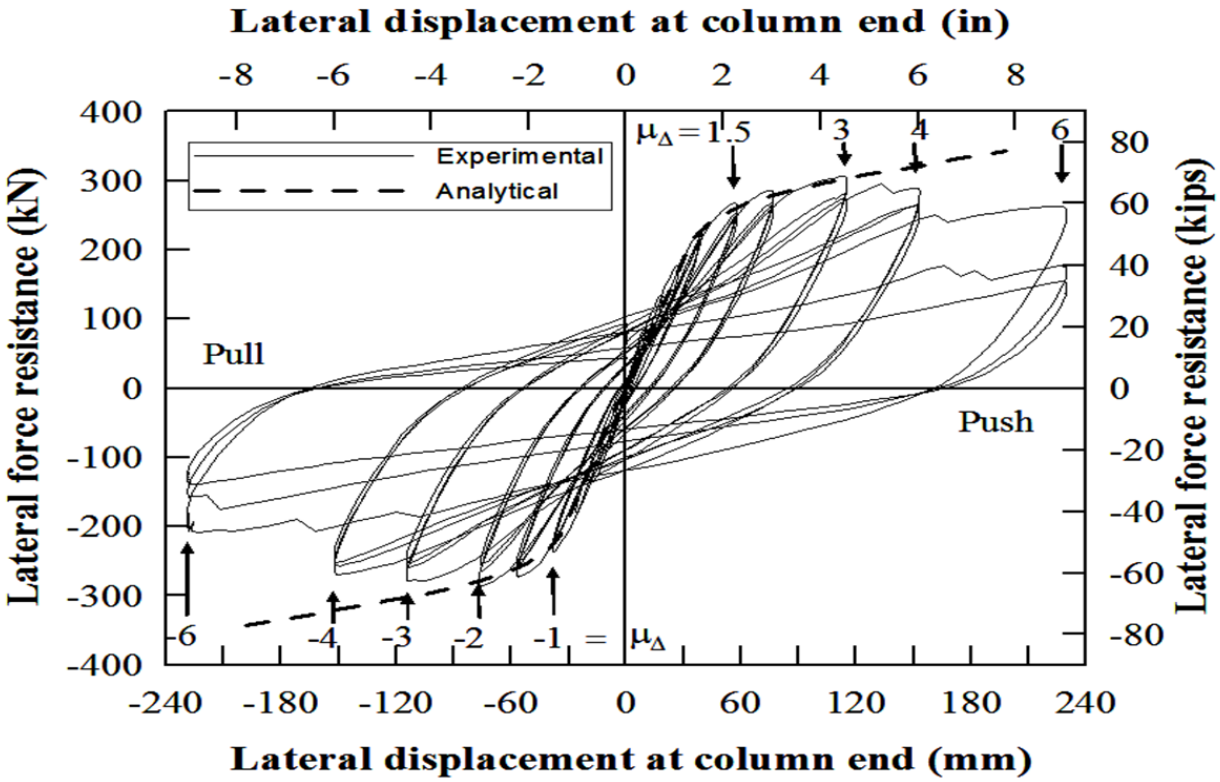
Lateral displacement at column end (in)
-8 -6 -4 -2 0 2 4 6 8
Lateral force resistance (kN)
400 300 200 100 0 -100 -200 -300 -400
Lateral force resistance (kips)
80 60 40 20 0 -20 -40 -60 -80
Experimental
Analytical
μΔ = 1.5 3 4 6
Pull
Push
-6 -4 -3 -2 -1 = μΔ
-240 -180 -120 -60 0 60 120 180 240
Lateral displacement at column end (mm)

Fig. 7d

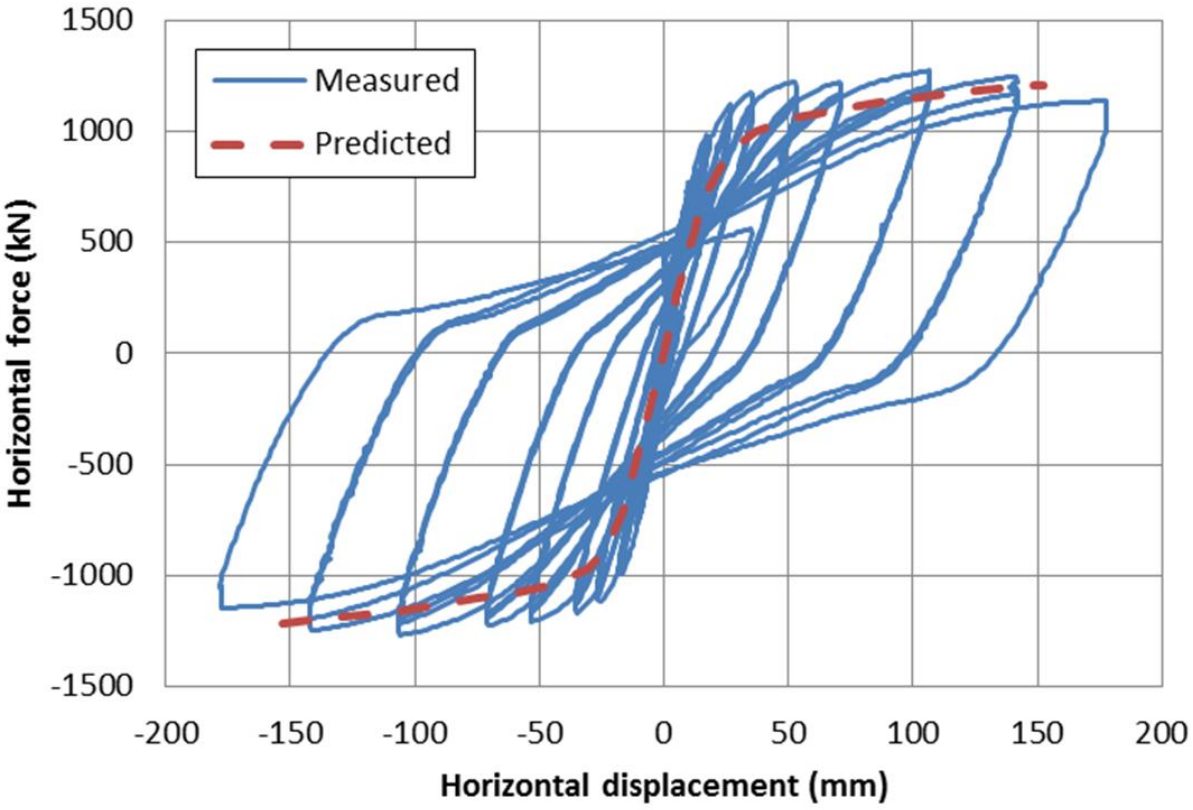
Measured
Predicted
Horizontal force (kN)
1500
1000
500
0
-500
-1000
-1500
-200
-150
-100
-50
0
50
100
150
200
Horizontal displacement (mm)

Fig. 8

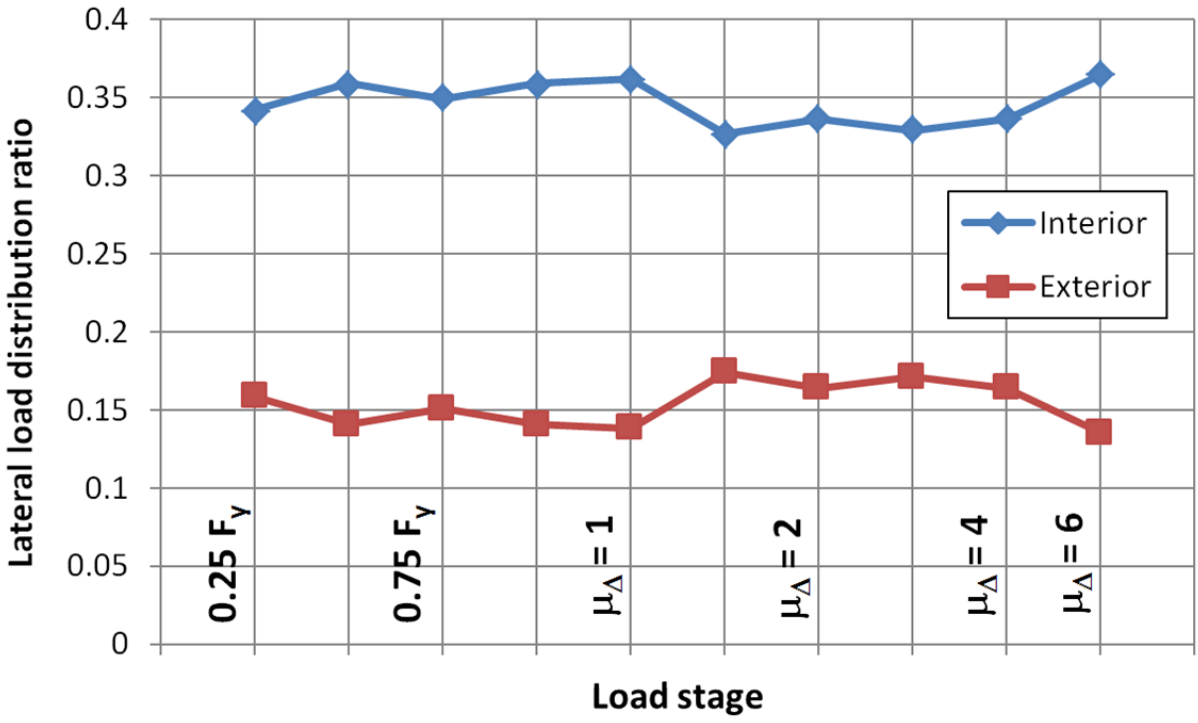
Lateral load distribution ratio
0.4
0.35
0.3
0.25
0.2
0.15
0.1
0.05
0
Interior
Exterior
0.25 Fy
0.75 Fy
μΔ = 1
μΔ = 2
μΔ = 4
μΔ = 6
Load stage

Fig. 9a

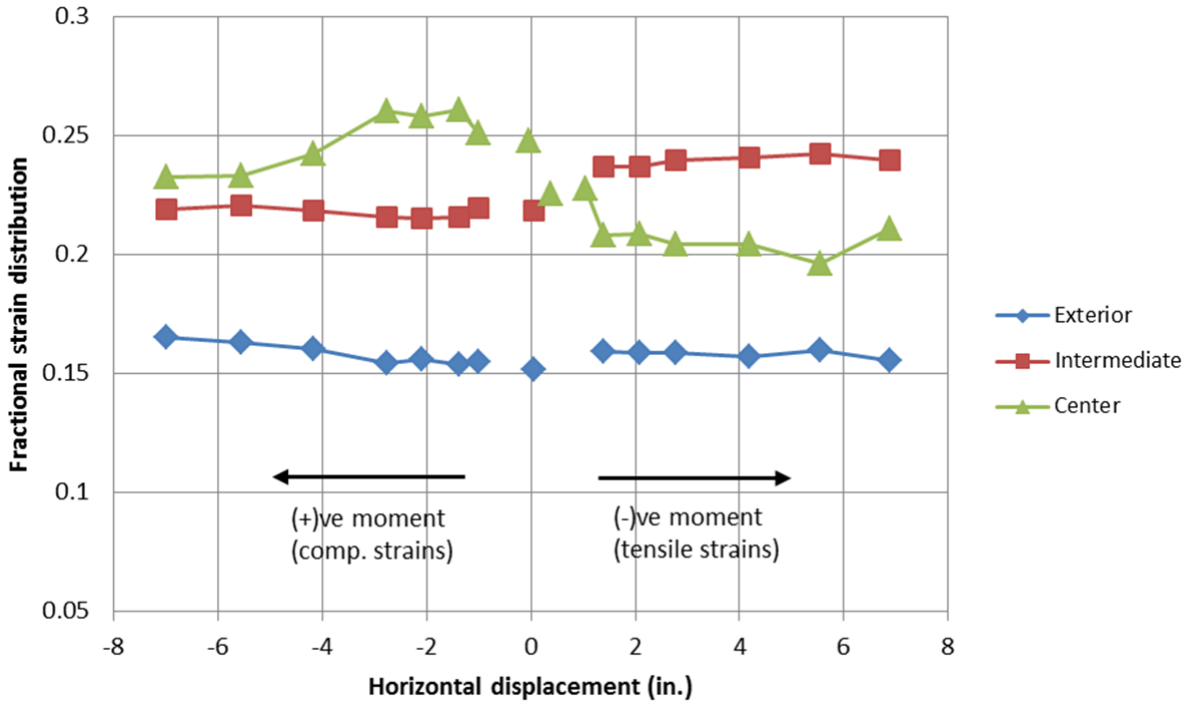
Fractional strain distribution
0.3
0.25
0.2
0.15
0.1
0.05
-8
-6
-4
-2
0
2
4
6
8
(+)ve moment
(comp. strains)
(-)ve moment
(tensile strains)
Horizontal displacement (in.)
Exterior
Intermediate
Center

Fig. 9b

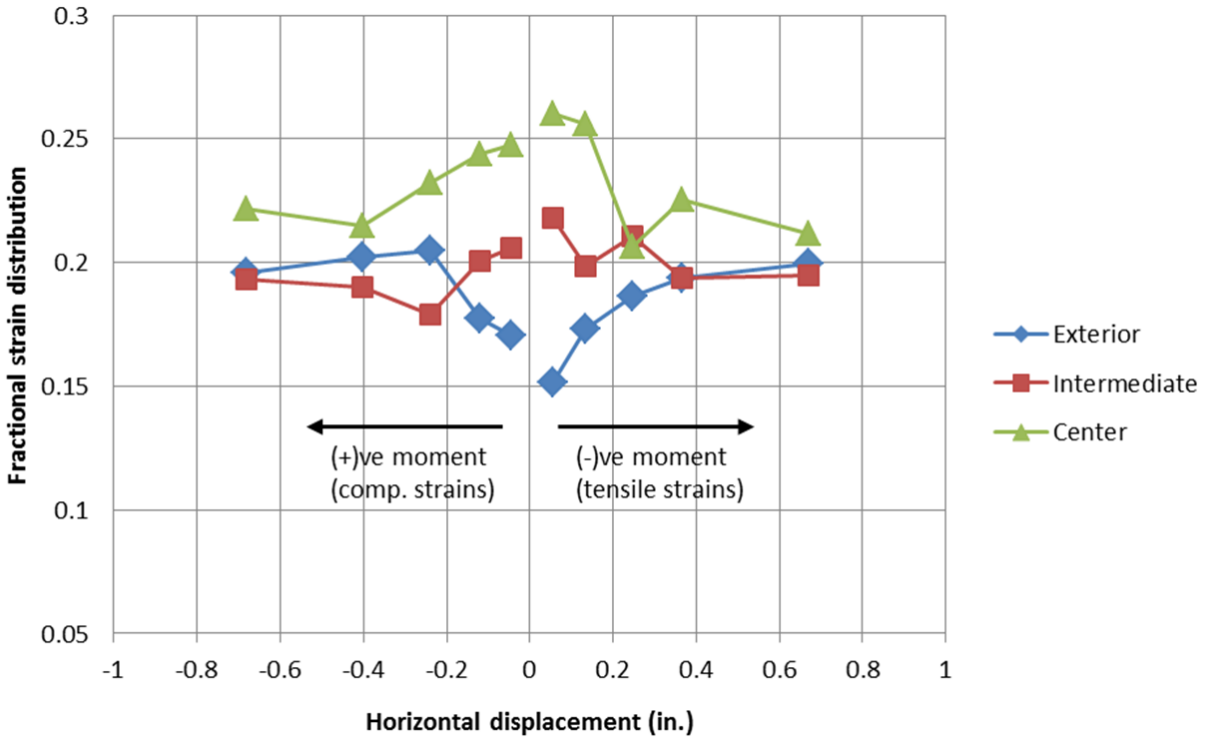
Fractional strain distribution
0.3
0.25
0.2
0.15
0.1
0.05
-1
-0.8
-0.6
-0.4
-0.2
0
0.2
0.4
0.6
0.8
1
Horizontal displacement (in.)
(+)ve moment
(comp. strains)
(-)ve moment
(tensile strains)
Exterior
Intermediate
Center

Fig. 10

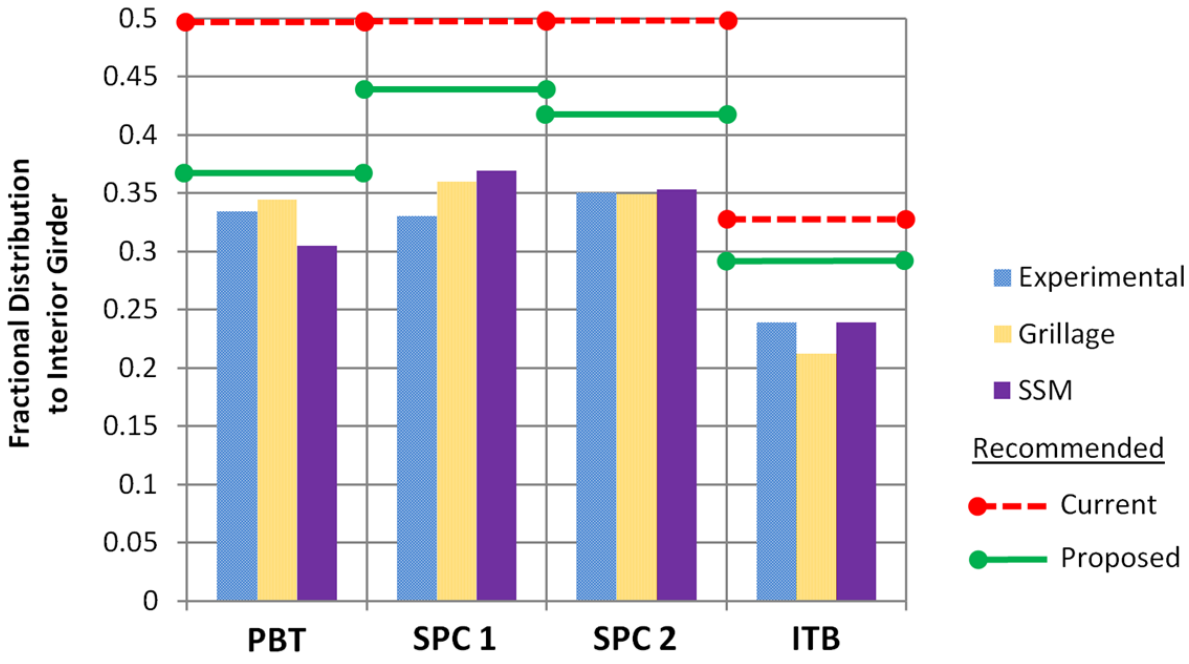
Fractional Distribution to Interior Girder
0.5
0.45
0.4
0.35
0.3
0.25
0.2
0.15
0.1
0.05
0
PBT
SPC 1
SPC 2
ITB
Experimental
Grillage
SSM
Recommended
Current
Proposed